

Article

The Effect of Conserved Histidine on the Proximity of Fe-S Clusters in Adenosine-5'-Phosphosulfate Reductases from *Pseudomonas aeruginosa* and *Enteromorpha intestinalis*

Jung-Sung Chung ^{1,2,*} , Sung-Kun Kim ³  and Thomas Leustek ⁴¹ Department of Agronomy, Gyeongsang National University, Jinju 52828, Republic of Korea² Institute of Agriculture and Life Science, Gyeongsang National University, Jinju 52828, Republic of Korea³ Department of Natural Sciences, Northeastern State University, 600 North Grand Avenue, Tahlequah, OK 74464, USA; kim03@nsuok.edu⁴ Biotechnology Center for Agriculture and the Environment, Department of Plant Biology and Pathology, Rutgers University, New Brunswick, NJ 08901, USA

* Correspondence: jschung@gnu.ac.kr; Tel.: +82-55-772-1876; Fax: +82-55-772-1879

Abstract: This study investigates the impact of conserved histidine (His) residue mutations on the adenosine 5'-phosphosulfate (APS) reductase enzymes *Pseudomonas aeruginosa* APR (PaAPR) and *Enteromorpha intestinalis* APR (EiAPR), focusing on the effects of His-to-alanine (Ala) and His-to-arginine (Arg) substitutions on enzyme activity, iron–sulfur [4Fe-4S] cluster stability, and APS binding affinity. Using recombinant His-tagged wild-types (WTs) and variants expressed in *Escherichia coli*, analyses revealed that both PaAPR and EiAPR enzymes exhibit a distinct absorption peak associated with their [4Fe-4S] clusters, which are critical for their catalytic functions. Notably, the His-to-Ala variants displayed reduced enzymatic activities and lower iron and sulfide contents compared to their respective WTs, suggesting alterations in the iron–sulfur cluster ligations and thus affecting APS reductase catalysis. In contrast, His-to-Arg variants maintained similar activities and iron and sulfide contents as their WTs, highlighting the importance of a positively charged residue at the conserved His site for maintaining structural integrity and enzymatic function. Further kinetic analyses showed variations in V_{max} and K_m values among the mutants, with significant reductions observed in the His-to-Ala variants, emphasizing the role of the conserved His in enzyme stability and substrate specificity. This study provides valuable insights into the structural and functional significance of conserved His residues in APS reductases, contributing to a better understanding of sulfur metabolism and its regulation in bacterial and plant systems. Future investigations into the structural characterization of these enzymes and the exploration of other critical residues surrounding the [4Fe-4S] cluster are suggested to elucidate the complete mechanism of APS reduction and its biological implications.

Keywords: adenosine 5'-phosphosulfate reductase; enzyme activity; histidine substitution; iron–sulfur cluster



Citation: Chung, J.-S.; Kim, S.-K.; Leustek, T. The Effect of Conserved Histidine on the Proximity of Fe-S Clusters in Adenosine-5'-Phosphosulfate Reductases from *Pseudomonas aeruginosa* and *Enteromorpha intestinalis*. *Microbiol. Res.* **2024**, *15*, 457–467. <https://doi.org/10.3390/microbiolres15020031>

Academic Editor: Juan Ayala

Received: 3 March 2024

Revised: 26 March 2024

Accepted: 28 March 2024

Published: 30 March 2024



Copyright: © 2024 by the authors. Licensee MDPI, Basel, Switzerland. This article is an open access article distributed under the terms and conditions of the Creative Commons Attribution (CC BY) license (<https://creativecommons.org/licenses/by/4.0/>).

1. Introduction

Inorganic sulfur is assimilated by plants, which then metabolize it into organosulfur compounds necessary for plant growth, development, and stress alleviation. Plants and microbes give vital molecules to animals, including humans, such as the amino acid methionine, which cannot be produced. Furthermore, numerous sulfur-containing metabolites have been shown to have health-promoting and protective effects on human bodies. As a result, a sufficient supply of sulfur can significantly impact crop output and the generation of beneficial phytochemicals [1–3].

Sulfur uptake and assimilation are necessary for cellular metabolism, plant growth and development, and responses to biotic and abiotic stressors in plants [4,5]. Plants

begin assimilation by activating sulfate with adenosine 5'-phosphosulfate (APS), catalyzed by the enzyme ATP sulfurylase. In a glutathione-dependent process, adenosine 5'-phosphosulfate reductase (APR) catalyzes the reduction of APS to sulfite. Sulfite reductase, which is ferredoxin-dependent, produces sulfides from sulfites. O-acetyl serine (OAS) thiol-degrading enzyme catalyzes the reaction of sulfides with OAS to form cysteine. OAS is produced by serine acetyltransferase [4,6,7]. Cysteine can be incorporated directly into proteins or further converted to methionine or glutathione, tripeptides with essential roles in oxidative stress defense, sulfur assimilation regulation, etc., [8]. Cysteine synthesis is thus a central point of cellular metabolism as this reaction interconnects sulfate, nitrate, and carbon assimilation [7].

Plant-type APS reductase (APR) consists of two domains: an amino-terminal reductase domain and a C-terminal glutaredoxin (GRX)-like domain that serves as an entry point for electrons in glutathione (GSH). The ability of plant APS reductase to use GSH as an electron donor is thought to depend on its carboxy-terminal domain, as is observed for thioredoxin (Trx) and Grx [9]. However, unlike the plant type, the bacterial form of APR contains just an N-terminal reductase domain and no C-terminal domain [9–12]. The N-terminal reductase domain of these two forms of APR contains a single [4Fe-4S] cluster [13,14]. According to recent data, the [4Fe-4S] cluster observed in APR does not act as an electron transporter, and its specific role is still unknown [15–17]. It has been revealed that most bacteria and higher plants' APRs contain [4Fe-4S] clusters and are associated with four cysteine ligands [17,18]. However, *Pseudomonas aeruginosa* APR (PaAPR), *Lemna minor* APR (LmAPR), *Arabidopsis thaliana* APR2 (AtAPR2), and *Enteromorpha intestinalis* APR (EiAPR) are consistent with a [4Fe-4S] cluster in which only three of the ligands to Fe are cysteine residues in these proteins [11,19,20].

In site-directed mutagenesis, the selection of replacement amino acids is critically guided by considerations of the protein's structure, function, and stability. The overarching stability of a protein is determined by a delicate equilibrium of internal forces, encompassing hydrophobic interactions, hydrogen bonds, van der Waals forces, and electrostatic interactions. The introduction of charged amino acids in place of neutral ones, or vice versa, can disrupt this balance, leading to repulsion forces or unintended attractions that compromise the native structure of the protein. As a result, in this study, we use the strategy of replacing positively charged amino acids with other amino acids with similar positive charges as uncharged amino acids to mitigate rapid changes in the structural and functional stability of proteins upon mutation.

As shown in Figure 1, one specific histidine residue exists close to the [4Fe-4S] cluster of PaAPR and is highly conserved (Figure 2). In this study, we prepared variants of both PaAPR and EiAPR, in which this conserved amino acid was replaced. Therefore, this study was performed to characterize the role of this conserved histidine in APRs of bacterial and plant types.

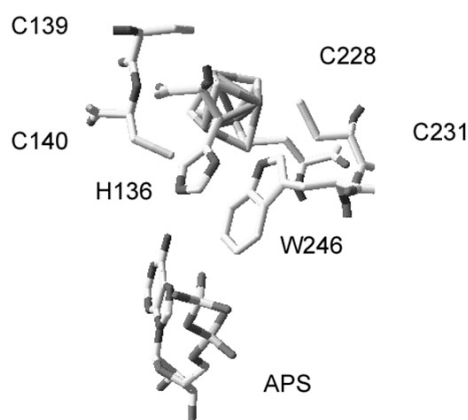


Figure 1. The structure of the [4Fe-4S] cluster region of PaAPR with a portion of a non-covalently bound APS molecule (taken from [17]).

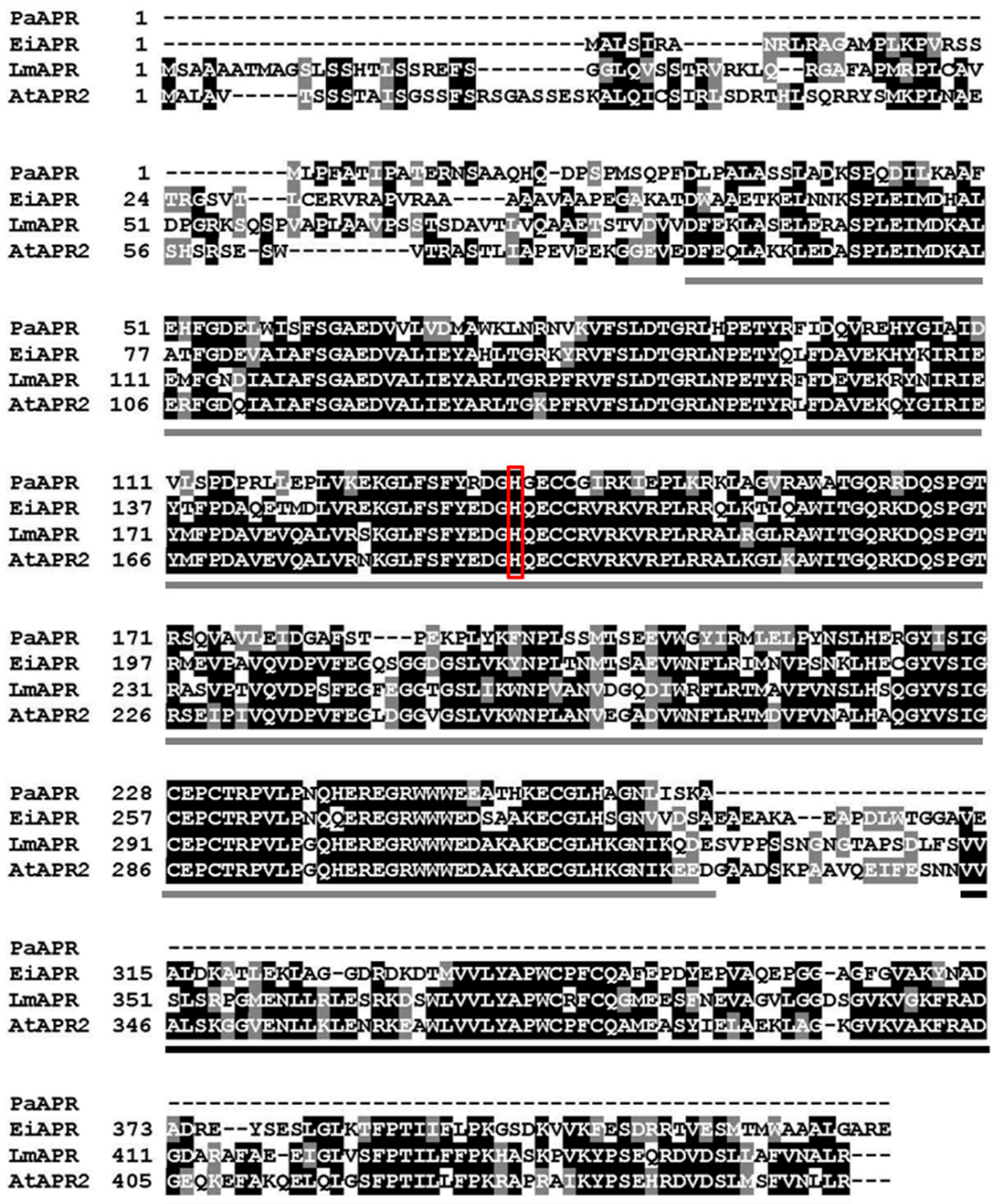


Figure 2. Comparison of amino acid sequences of PaAPR, EiAPR, LmAPR, and AtAPR2. Alignment was shaded with a 100% threshold to determine the strictly conserved residues. The gray and black shading shows the approximate location of the reductase domain and C-terminal (Trx/Grx-like) domain, respectively. The mutated conserved amino acids are identified by the red box.

2. Materials and Methods

2.1. Plasmid, Site-Directed Mutagenesis, and Recombinant Protein Expressions

The pET30b-PaAPR and pET30b-EiAPR [14,21] constructs were used as templates for site-specific mutagenesis. The QuikChange kit was used to create site-specific mutations in

PaAPR and EiAPR (Stratagene, La Jolla, CA, USA). Table 1 contains the primer sequences used to create each mutant. At Texas Tech University's Biotechnology Core Facility, the sequences of the genes encoding these variations were validated by DNA sequencing. Wild-type (WT) and variants of PaAPR and EiAPR were expressed in the Rosseta2 (DE3) (Navagen, Foster, CA, USA) *E. coli* strain.

Table 1. Sequences of oligonucleotide primers used in site-directed mutagenesis PCR amplification. Bold indicates the target amino acid sequence.

Gene	Primer	Sequence 5'-3'	Mutated Codon
PaAPR	H136A For	TTC TAC CGG GAC GGC GCC GGC GAG TGC TGC GGC	CAC→GCC
	H136A Rev	GCC GCA GCA CTC GCC GGC GCC GTC CCG GTA GAA	
	H136R For	TTC TAC CGG GAC GGC CGC GGC GAG TGC TGC GGC	CAC→CGC
	H136R Rev	GCC GCA GCA CTC GCC GCG GCC GTC CCG GTA GAA	
EiAPR	H162A For	TTC TAC GAG GAC GGC GCC CAA GAG TGC TGC CGC	CAT→GCC
	H162A Rev	GCG GCA GCA CTC TTG GGC GCC GTC CTC GTA GAA	
	H162R For	TTC TAC GAG GAC GGC CGC CAA GAG TGC TGC CGC	CAT→CGC
	H162R Rev	GCG GCA GCA CTC TTG GCG GCC GTC CTC GTA GAA	

2.2. Recombinant Protein Expression and Purification

WT PaAPR and EiAPR and variants were prepared and purified as described previously [14,22]. The *E. coli*, Roseta2 (DE3) strain cultures were grown to an optical density of 0.6 at 600 nm at 37 °C in Luria–Bertani (LB) medium containing 50 mg/L of kanamycin and 34 mg/L of chloramphenicol. Isopropyl β-D-thiogalactopyranoside (IPTG) was then added to a final concentration of 1 mM and grown at 30 °C in LB medium for 16 h. After induction by IPTG, *E. coli* Rosseta2 (DE3) cells were harvested, broken using a French press, and centrifuged. The supernatant was filtered through a 0.45 μm pore-size membrane and applied to a Ni²⁺ affinity column (Hi-Trap Chelating HP, obtained from Amersham Biosciences) incorporated into a BioCAD perfusion chromatography system (PerSeptive BioSciences). All protein samples used in this study showed a single Coomassie blue staining band after polyacrylamide gel electrophoresis in the presence of sodium dodecyl sulfate [23].

2.3. Iron Contents

Total iron contents were measured as described by Massey (1957) using ferric ammonium sulfate as a standard [24]. To conduct the experiment, start by preparing a sample with a concentration of 20–40 nmol. Then, add 5% trichloroacetic acid (TCA) to the sample to achieve a total volume of 0.4 mL. After adding the TCA, thoroughly mix the solution and centrifuge it at 10,000 rpm for 5 min. Following centrifugation, carefully transfer the supernatant to a new tube to separate it from any precipitate. Next, add 0.36 mL of clean water to the supernatant to dilute it. Follow this by adding 0.15 mL of 0.1% o-phenanthroline, which will serve as a developing agent for the reaction. Then, introduce 0.04 mL of 0.12 N ascorbate to the mixture as a reducing agent. After the ascorbate, add 0.05 mL of saturated ammonium acetate, which will help in adjusting the pH and stabilizing the solution. Once all reagents have been added, allow the mixture to incubate at room temperature for one hour to ensure that the reaction proceeds to completion. Finally, measure the absorbance of the resulting solution at 510 nm using a spectrophotometer to assess the outcome of the experiment.

2.4. Sulfide Contents

Acid-labile sulfide was determined as described by King and Morris (1967) [25]. Add 1.5 mL of zinc-alkaline solution to a 10 mL test tube fitted with a cap. Then, quickly add 2.0 mL of the sample, which should contain 5 to 20 nanomoles of sulfide, into the test tube. Immediately seal the tube with the cap after adding the sample. Incubate the sealed test

tube at room temperature for 1 h. Subsequently, add 0.3 mL of 0.02 M N,N'-dimethyl-p-phenylenediamine sulfate in 7.2 N hydrochloric acid (HCl) to the mixture, followed by the addition of 0.3 mL of 0.03 M ferric chloride (FeCl₃) dissolved in 1.2 N HCl. After incorporating all the reagents, incubate the test tube once more at room temperature for 20 min. Finally, measure the absorbance of the solution at 670 nm using a spectrophotometer.

2.5. Enzyme Activity Assay

The enzymatic activities of PaAPR (and its variants) and EiAPR (and its variants) were measured using two different coupled enzyme assays. In the first assay, the activity of PaAPR in the presence of *E. coli* thioredoxin is assessed by linking the oxidation of thioredoxin, catalyzed by PaAPR, to its subsequent reduction by NADPH, a reaction facilitated by *E. coli* NADPH thioredoxin reductase (NTR). The reaction mix for this assay includes a Tris-HCl buffer (pH 8.5), EDTA, sodium sulfate, APS (as a potential substrate or electron acceptor), *E. coli* NTR, β -NADPH, PaAPR, and varying concentrations of *E. coli* thioredoxin. The second assay measures the activity of EiAPR using a similar approach but focuses on the oxidation of glutathione (GSH), which is then reduced back by NADPH with the aid of yeast glutathione reductase (GR). The mix for this assay also comprises Tris-HCl buffer, EDTA, sodium sulfate, APS, GR, β -NADPH, EiAPR, and different concentrations of glutathione. In both setups, the consumption of NADPH is monitored by observing decreases in absorbance at 340 nm, a method that quantifies the enzymatic activity. These rates of NADPH oxidation are calculated per minute and analyzed using an extinction coefficient specific to NADPH. Microsoft Excel 2019 is employed to process the data according to the Michaelis–Menten model, which helps in understanding the kinetic properties of the enzymes, such as their efficiency and substrate affinity, by providing parameters like V_{max} (maximum velocity) and K_m (substrate concentration at half V_{max}).

2.6. Binding Assay

Formation of non-covalent complexes between APR enzyme and the substrate APS ranges in absorbance in the visible region of the spectrum that occurred when they were mixed. Changes in absorbance were measured at 0.5 nm spectral resolution, using a Shimadzu Model UV-2401 PC spectrophotometer (Kyoto, Japan), as described previously for other protein/protein complexes [26]. Difference spectra of the complex minus the sums of the spectra of the components of the complexes were obtained by computer subtraction as described previously [26].

2.7. Statistical Analysis

Statistical analyses were conducted to obtain the arithmetic mean and standard error, and the significance of differences among the variants was evaluated using one-way ANOVA, complemented by Tukey's HSD test for significance levels of $p < 0.05$ and $p < 0.01$. These statistical procedures were performed using Microsoft Excel 2019.

3. Results and Discussion

3.1. Molecular Cloning and Protein Expression and Purification

The construct used to express the WT forms of PaAPR and EiAPR in *E. coli* was designed to have a 6-histidine (His) extension at the N-terminus to facilitate purification of the enzyme from soluble *E. coli* extract using a Ni²⁺ affinity column. SDS-PAGE analysis of freshly prepared samples of His-tagged, recombinant PaAPR and its variants showed a single major coomassie-staining band with an apparent molecular mass of 35 kDa, and analysis of His-tagged, recombinant EiAPR and its variants produced a single major coomassie-staining band with an apparent molecular mass of 48 kDa.

3.2. Protein Spectra, and Iron and Sulfur Contents

The spectra of PaAPR and EiAPR WTs included a broad peak with a maximum of 386 nm, as previously described [14,15]. A single [4Fe-4S]₂⁺ cluster has been demonstrated to give rise to this absorbance feature [14,15]. All His to arginine (Arg) variants of PaAPR and EiAPR contained a broad peak similar to WT PaAPR and EiAPR, respectively (data not shown). However, the peak at 281 nm and the broad absorbance centered at 385 nm was slightly lower in the His to alanine (Ala) variants of PaAPR and EiAPR than in each WT (data not shown). Table 2 shows non-heme iron and acid-labile sulfide contents for freshly prepared WTs and His-variants. Both WTs' iron and sulfide contents have been reported [14,15]. WT PaAPR contained 3.95 ± 0.08 mol of iron and 3.58 ± 0.3 mol of sulfide per mole of the enzyme (Table 2), and WT EiAPR contained 3.76 ± 0.03 mol of iron and 3.44 ± 0.63 mol of sulfide per mol of the enzyme. Notably, the iron and sulfide contents of the H162A variant were lower than those of WT EiAPR (Table 2).

Table 2. Analysis of iron and acid-labile sulfide contents.

	Variant	Sulfide Content (nmol/nmol of Protein)	Iron Content (nmol/nmol of Protein)
PaAPR	Wild-type	3.58 ± 0.30^a	3.95 ± 0.08^a
	H136A	2.51 ± 0.06^b	3.25 ± 0.30^b
	H136R	3.32 ± 0.38^a	3.93 ± 0.08^a
EiAPR	Wild-type	3.44 ± 0.63^a	3.76 ± 0.03^a
	H162A	2.14 ± 0.48^b	2.91 ± 0.33^b
	H162R	3.37 ± 0.20^a	3.86 ± 0.07^a

Different lowercase letters show significant differences between wild-type and variants of PaAPR and EiAPR, as calculated using Tukey's test.

3.3. PaAPR and Variant Activity and Kinetic Analysis

Figure 3 shows the Trx dependence of WT and variant PaAPR activities as measured by the NADPH/NTR-coupled assay technique described in Section 2 and Table 3 summarizes the steady-state kinetic properties of WT PaAPR and its variants. The steady-state characteristics of an H136R variation in which a positive charge on Arg replaced the positive charge on His were highly similar to the WT. However, an H136A variant replaced by the uncharged Ala decreased in V_{max} by about 16% points compared with WT PaAPR. In addition, the V_{max} of H136R, which was replaced with positively charged Arg, was not significantly different from that of the WT. The dissociation constant of APS was determined using spectrophotometric titration to see if His/Ala and His/Arg variations altered binding to these substrates. The dissociation constant (K_d) values were examined for noticeable spectrum shifts in the visible area between 386 and 650 nm, indicating the formation of a complex between the enzyme and the substrate APS. Table 3 also summarizes the K_d values for binding WT PaAPR and mutants to APS, all measured using the spectral perturbation protocol previously described [11]. In WT PaAPR, the K_d value for APS was measured to be 20 μM. However, the K_d value for APS in H136A was double that of the WT, similar to WT H136R.

3.4. EiAPR and Variants Activity and Kinetic Analysis

Figure 4 depicts the glutathione dependence of EiAPR WT and variant activities as measured by the NADPH/GR-coupled assay setup described in Section 2 and Table 4 depicts the steady-state kinetic parameters of WT EiAPR and His-variants. Compared to WT EiAPR, H162A showed a 52% lower V_{max}, but H162R had no significant difference in V_{max} (Table 4). The K_m values of the H162A and H162R variants, on the other hand, were 2.5 and 2.2 times higher than WT EiAPR, respectively (Table 4). The K_d value for APS of WT EiAPR was 20 μM, and the K_d value for APS of the H162A mutant of EiAPR was two-fold higher than that of WT EiAPR. In addition, the H162R variant had slightly lower V_{max} and K_d values for APS than the wild type, but there was no significant difference.

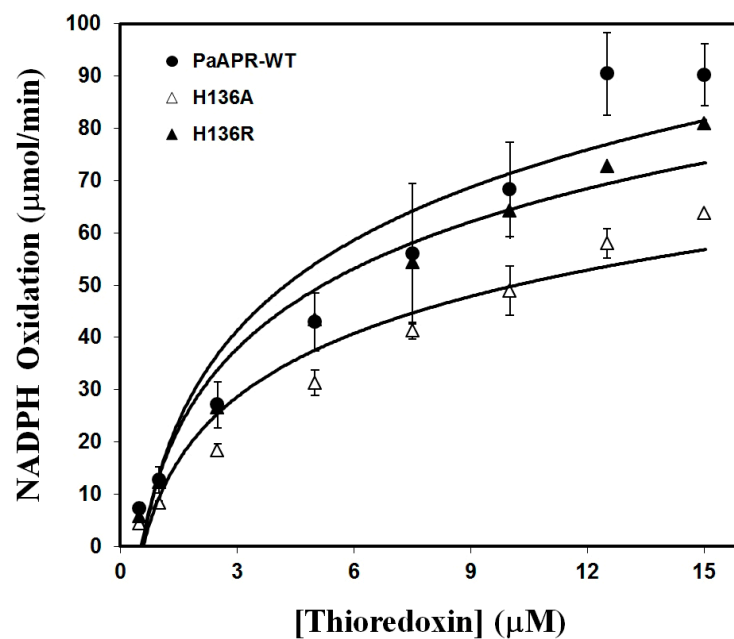


Figure 3. The activity of PaAPR and variants with *E. coli* Trx. PaAPR activity was measured using the NADPH/NTR-coupled assay system at 100 μ M APS. WT, wild-type.

Table 3. The kinetic parameters and binding constants for PaAPR and variants with wild-type *E. coli* thioredoxin.

	Variant	Relative V_{max} *	K_m (μ M)	K_d (μ M) (APS)
PaAPR	Wild-type	100.00 \pm 11.57 ^a	8.33 \pm 1.65 ^a	20 ^a
	H136A	84.66 \pm 3.07 ^b	10.55 \pm 0.78 ^b	70 ^b
	H136R	102.46 \pm 8.60 ^a	8.55 \pm 2.05 ^a	14.8 ^a

* This value 100% corresponds to a rate of 0.68 μ mol of NADPH oxidized/min/ μ g of PaAPR. Different lowercase letters show significant differences between wild-type and variants, as calculated using Tukey's test.

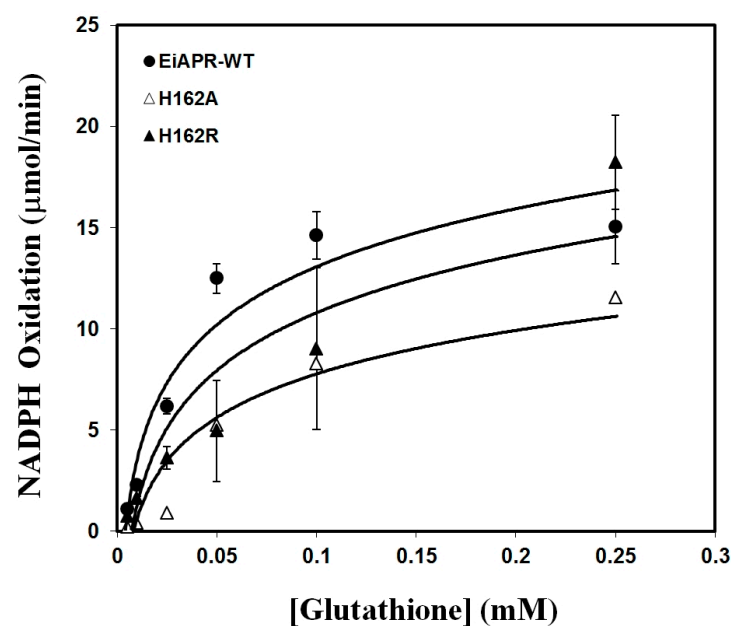


Figure 4. The activity of EiAPR variants with GSH. EiAPR activity was measured using the NADPH/GR-coupled assay system at 100 μ M APS. WT, wild-type.

Table 4. The kinetic parameters and binding constants for EiAPR and variants with glutathione.

	Variant	Relative V_{max} *	K_m (μM)	K_d (μM) (APS)
EiAPR	Wild-type	100.00 \pm 32.68 ^a	83.35 \pm 23.55 ^a	20 ^a
	H162A	48.06 \pm 15.68 ^b	204.15 \pm 5.87 ^b	40 ^b
	H162R	83.18 \pm 13.07 ^a	183.35 \pm 23.55 ^b	32 ^a

* The value 100% corresponds to a rate of 0.11 μmol of NADPH oxidized/min/ μg of EiAPR. Different lowercase letters show significant differences between wild-type and variants, as calculated using Tukey's test.

3.5. Histidine Substitutions in APS Reductase: Activity and Binding Impacts

The choice to focus research on a conserved histidine residue close to the [4Fe-4S] cluster in APR (APS reductase) from both bacterial and plant sources stems from several key considerations that highlight the potential significance of this residue in the enzyme's function, structure, and electron transfer mechanisms. The fact that the histidine residue is highly conserved across different species, including both bacterial and plant forms of APR, suggests that it plays a critical role in the enzyme's function. Evolutionary conservation is a strong indicator of functional importance, as amino acids crucial to protein structure or function tend to be preserved throughout evolution. The physical closeness of the histidine to the [4Fe-4S] cluster is particularly intriguing. The [4Fe-4S] cluster is a cofactor known to play essential roles in various electron transfer reactions and in the catalytic activity of enzymes. Although in the case of APR, the [4Fe-4S] cluster does not act as an electron transporter, its presence and the proximity of the conserved histidine suggest a potential interaction that could be vital for the enzyme's structure, stability, or function. Histidine residues can play diverse roles in proteins, including serving as ligands for metal ions, participating in catalytic activities, and contributing to protein stability. Their side chains are capable of forming hydrogen bonds and participating in coordination with metal clusters, which could be crucial in maintaining the integrity and proper positioning of the [4Fe-4S] cluster within the enzyme. Even though the cluster in APR is not involved in electron transfer, understanding the role of nearby residues like histidine could provide insights into alternative functions of the cluster or reveal new mechanisms of action for the enzyme.

Kim et al. previously investigated the roles of three cysteine residues, that is, C139, C228, and C231 in PaAPR and C166, C257, and C260 in EiAPR, which served as ligands for the [4Fe-4S] cluster [14,15]. The other two cysteines (C140 and C256 in PaAPR; C165 and C285 in EiAPR) function as a redox-active disulfide/dithiol couple at the site for entry of reducing equivalents into the enzyme from their physiological electron donor. It has been reported that serine-substituted variants of three cysteines that previously ligated [4Fe-4S] clusters contained less iron and sulfides, suggesting a loss of Cys-released S and/or Fe [14,15]. However, their activities were not determined, and these are required for the iron-sulfur cluster. Previously reported site-directed experiments performed with the AtAPR2 and LmAPR provided evidence that three cysteines present in the plant enzyme are involved in linking iron-sulfur clusters [20].

This study demonstrates that the activity of the enzyme replaced by Ala with conserved histidine in proximity to the iron-sulfur cluster of bacterial and plant-type APS reductase is lower than that of both WTs. Furthermore, iron and sulfide contents of His variants of both PaAPR and EiAPR, which changed to Ala, were lower than those of the WTs. However, there was no significant difference in iron and sulfide content and enzyme activity in the variants of PaAPR and EiAPR in which the conserved His was changed to the positively charged amino acid Arg. Thus, this investigation indicates that conserved His replacement with uncharged Ala affected iron-sulfur cluster ligation and APS reductase enzyme catalysis. Significantly, the iron-sulfur cluster cofactor in APR enhances APS reduction and plays a pivotal role in substrate specificity and catalysis [27].

In particular, in the structure of PaAPR, His136 is located very close to the [4Fe-4S] cluster inside the enzyme. In particular, in the structure of PaAPR, His136 is located very

close to the iron–sulfur cluster inside the enzyme. The His/Ala variant is predicted to affect the enzyme activity or the binding of the substrate APS due to the change in the internal space. Another possibility is that the interaction between the conserved His and its surrounding amino acids may change the enzyme's structure or affect the binding of the substrate, thereby affecting the activity of the enzyme. Moreover, the results for the enzymatic activity of the His/Arg variants are similar to both WTs, indicating that a positively charged amino acid is required for the structure or activity of the enzyme at the conservative His position. The His/Ala variant of the EiAPR plant type decreased by about 50% compared to the WT in the enzyme activity, and the His/Ala variant of the PaAPR bacterial type decreased by about 15% compared to the WT. Differences in enzyme activity between bacterial and plant types showed similar results for iron and sulfur content. Therefore, these results imply that the conservative His (i.e., H136 of PaAPR and H162 of EiAPR) does not bind directly to the [4Fe-4S] cluster but affects the structure and activity of APS reductase.

In addition, although the structure of the plant-type APR has not been identified yet, the amino acid sequence of the reductase domain is very similar to that of PaAPR, whose tertiary structure of the protein has been revealed [17]; therefore, their tertiary structure is expected to be similar. However, the structural characteristics of the unstable enzyme of the His/Ala variant of EiAPR influenced the enzyme catalysis more than the His/Ala variant of the bacterial-type PaAPR. This means that the role of H162 in the plant-type EiAPR is more critical than that of the bacterial type in the structural stability and catalysis of enzymes related to the binding of iron–sulfur clusters. The features of APS reductase, which play a significant role in sulfur metabolism, will be better understood in future studies if more studies of other amino acids around the iron–sulfur cluster, including the conserved His, are carried out.

4. Conclusions

APR is an essential enzyme in sulfur metabolism. The iron–sulfur cluster of APR is a crucial part of the enzyme's structural and catalytic mechanisms, but its exact function is unknown. The role of His amino acid, which is conserved in bacterial and plant-type APRs and is found close to the iron–sulfur cluster, was explored in this study. In both types, replacing the conserved amino acid His with uncharged Ala resulted in lower iron and sulfur levels, as well as decreased enzyme activity. Moreover, APRs of the plant type had a more significant impact on Ala substitution of His than APRs of the bacterial type. However, the iron and sulfur levels and enzyme activity were barely altered when His was replaced with Arg, which is the same positive charge. These findings demonstrate that a positively charged amino acid residue is required to conserve His position in the structural and catalytic mechanism of APR, with a greater significance in plant APR than in bacterial APR.

Author Contributions: Conceptualization, T.L. and J.-S.C.; methodology, J.-S.C. and S.-K.K.; formal analysis, J.-S.C. and S.-K.K.; Investigation, J.-S.C.; writing—original draft preparation, J.-S.C.; writing—review and editing, T.L. and S.-K.K.; All authors have read and agreed to the published version of the manuscript.

Funding: This research received no external funding.

Institutional Review Board Statement: Not applicable.

Informed Consent Statement: Not applicable.

Data Availability Statement: Data are contained within the article.

Conflicts of Interest: The authors declare no conflicts of interest.

Abbreviations

APS, adenosine 5'-phosphosulfate; Trx, thioredoxin; GSH, glutathione; PaAPR, *Pseudomonas aeruginosa* APS reductase; EiAPR, *Enteromorpha intestinalis* APS reductase; IPTG, isopropyl β -D-thiogalactopyranoside; NADPH, nicotinamide adenine dinucleotide phosphate; NTR, NADPH dependent thioredoxin reductase; and GR, glutathione reductase.

References

1. Takahashi, H.; Kopriva, S.; Giordano, M.; Saito, K.; Hell, R. Sulfur assimilation in photosynthetic organisms: Molecular functions and regulations of transporters and assimilatory enzymes. *Annu. Rev. Plant Biol.* **2011**, *62*, 157–184. [[CrossRef](#)] [[PubMed](#)]
2. Sauter, M.; Moffatt, B.; Saechao, M.C.; Hell, R.; Wirtz, M. Methionine salvage and S-adenosylmethionine: Essential links between sulfur, ethylene and polyamine biosynthesis. *Biochem. J.* **2013**, *451*, 145–154. [[CrossRef](#)] [[PubMed](#)]
3. Calderwood, A.; Kopriva, S. Hydrogen sulfide in plants: From dissipation of excess sulfur to signaling molecule. *Nitric Oxide.* **2014**, *41*, 72–78. [[CrossRef](#)] [[PubMed](#)]
4. Ravilious, G.E.; Jez, J.M. Structural biology of plant sulfur metabolism: From assimilation to biosynthesis. *Nat. Prod. Rep.* **2012**, *29*, 1138–1152. [[CrossRef](#)] [[PubMed](#)]
5. Saito, K. Sulfur assimilatory metabolism. The long and smelling road. *Plant Physiol.* **2004**, *136*, 2443–2450. [[CrossRef](#)]
6. Brunold, C. Reduction of sulfate to sulfide. In *Sulfur Nutrition and Sulfur Assimilation in Higher Plants: Fundamental, Environmental and Agricultural Aspects*; Rennenberg, H., Brunold, C., De Kok, L.J., Stulen, I., Eds.; SPB Academic Publishing: The Hague, Germany, 1990; pp. 13–31. ISBN 90-5103-038-X.
7. Kopriva, S.; Buchert, T.; Fritz, G.; Suter, M.; Benda, R.; Schunemann, V.; Koprivova, A.; Schurmann, P.; Trautwein, A.X.; Kroneck, P.M.; et al. The presence of an iron-sulfur cluster in adenosine 5'-phosphosulfate reductase separates organisms utilizing adenosine 5'-phosphosulfate and phosphoadenosine 5'-phosphosulfate for sulfate assimilation. *J. Biol. Chem.* **2002**, *277*, 21786–21791. [[CrossRef](#)]
8. Noctor, G.; Arisi, A.M.; Jouanin, L.; Kunert, K.J.; Rennenberg, H.; Foyer, C.H. Glutathione: Biosynthesis, metabolism and relationship to stress tolerance explored in transformed plants. *J. Exp. Bot.* **1998**, *49*, 623–647. [[CrossRef](#)]
9. Bick, J.A.; Åslund, F.; Chen, Y.; Leustek, T. Glutaredoxin function for the carboxyl terminal domain of the plant-type 5'-adenylyl sulfate (APS) reductase. *Proc. Natl. Acad. Sci. USA* **1998**, *95*, 8404–8409. [[CrossRef](#)] [[PubMed](#)]
10. Lillig, C.H.; Prior, A.; Schwenn, J.D.; Åslund, F.; Ritz, D.; Vlamis-Gardikas, A.; Holmgren, A. New thioredoxins and glutaredoxins as electron donors of 3'-phosphoadenylylsulfate reductase. *J. Biol. Chem.* **1999**, *274*, 7695–7698. [[CrossRef](#)]
11. Ravilious, G.E.; Nguyen, A.; Francois, J.A.; Jez, J.M. Structural basis and evolution of redox regulation in plant adenosine-5'-phosphosulfate kinase. *Proc. Natl. Acad. Sci. USA* **2012**, *109*, 309–314. [[CrossRef](#)]
12. Koprivova, A.; Kopriva, S. Sulfation pathways in plants. *Chem. Biol. Interact.* **2016**, *259*, 23–30. [[CrossRef](#)]
13. Weber, M.; Suter, M.; Brunold, C.; Kopriva, S. Sulfate assimilation in higher plants characterization of a stable intermediate in the adenosine 5'-phosphosulfate reductase reaction. *Eur. J. Biochem.* **2000**, *267*, 3647–3653. [[CrossRef](#)]
14. Kim, S.K.; Rahman, A.; Conover, R.C.; Johnson, M.K.; Mason, J.T.; Hirasawa, M.; Moore, M.L.; Leustek, T.; Knaff, D.B. Properties of the cysteine residues and the iron-sulfur cluster of the assimilatory 5'-adenylyl sulfate reductase from *Enteromorpha intestinalis*. *Biochemistry* **2006**, *45*, 5010–5018. [[CrossRef](#)]
15. Kim, S.K.; Rahman, A.; Bick, J.A.; Conover, R.C.; Johnson, M.K.; Mason, J.T.; Hirasawa, M.; Leustek, T.; Knaff, D.B. Properties of the cysteine residues and iron-sulfur cluster of the assimilatory 5'-adenylylsulfate reductase from *Pseudomonas aeruginosa*. *Biochemistry* **2004**, *43*, 13478–13486. [[CrossRef](#)]
16. Carroll, K.S.; Gao, H.; Chen, H.; Stout, C.D.; Leary, J.A.; Bertozzi, C.R. A conserved mechanism for sulfonucleotide reduction. *PLoS Biol.* **2005**, *3*, e250. [[CrossRef](#)]
17. Chartron, J.; Carroll, K.S.; Shiao, C.; Gao, H.; Leary, J.A.; Bertozzi, C.R.; Stout, C.D. Substrate recognition, protein dynamics, and iron-sulfur cluster in *Pseudomonas aeruginosa* adenosine-5'-phosphosulfate reductase. *J. Mol. Biol.* **2006**, *364*, 162–169. [[CrossRef](#)]
18. Feliciano, P.R.; Carroll, K.S.; Drennan, C.L. Crystal Structure of the [4Fe-4S] Cluster-Containing Adenosine-5'-phosphosulfate Reductase from *Mycobacterium tuberculosis*. *ACS Omega* **2021**, *6*, 13756–13765. [[CrossRef](#)]
19. Carroll, K.S.; Gao, H.; Chen, H.; Leary, J.A.; Bertozzi, C.R. Investigation of the iron-sulfur cluster in *Mycobacterium tuberculosis* APS reductase: Implications for substrate binding and catalysis. *Biochemistry* **2005**, *44*, 14647–14657. [[CrossRef](#)]
20. Kopriva, S.; Buchert, T.; Fritz, G.; Suter, M.; Weber, M.; Benda, R.; Schaller, J.; Feller, U.; Schurmann, P.; Schunemann, V.; et al. Plant adenosine 5'-phosphosulfate reductase is a novel iron-sulfur protein. *J. Biol. Chem.* **2001**, *276*, 42881–42886. [[CrossRef](#)]
21. Gao, Y.; Schofield, O.; Leustek, T. Characterization of sulfate assimilation in marine algae focusing on the enzyme 5'-adenylylsulfate (APS) reductase. *Plant Physiol.* **2000**, *123*, 1087–1096. [[CrossRef](#)]
22. Chung, J.S.; Noguera-Mazon, V.; Lancelin, J.M.; Kim, S.K.; Hirasawa, M.; Hologne, M.; Leustek, T.; Knaff, D.B. The Interaction Domain on Thioredoxin for *Pseudomonas aeruginosa* 5'-adenylylsulfate Reductase. *J. Biol. Chem.* **2009**, *284*, 31181–31189. [[CrossRef](#)] [[PubMed](#)]
23. Bradford, M.M. A rapid and sensitive method for the quantitation of microgram quantities of protein utilizing the principle of protein-dye binding. *Anal. Biochem.* **1976**, *72*, 248–254. [[CrossRef](#)] [[PubMed](#)]

24. Massey, V. Studies on succinic dehydrogenase: VII. Valency state of the iron in beef heart succinic dehydrogenase. *J. Biol. Chem.* **1957**, *229*, 763–770. [[CrossRef](#)] [[PubMed](#)]
25. King, T.E.; Morris, R.O. Determination of acid-labile sulfide and sulfhydryl groups. *Methods Enzymol.* **1967**, *10*, 634–641. [[CrossRef](#)]
26. Srivastava, A.P.; Knaff, D.B.; Sétif, P. Kinetic studies of a ferredoxin-dependent cyanobacterial nitrate reductase. *Biochemistry* **2014**, *53*, 5092–5101. [[CrossRef](#)]
27. Bhave, D.P.; Hong, J.A.; Keller, R.L.; Krebs, C.; Carroll, K.S. Iron-sulfur cluster engineering provides insight into the evolution of substrate specificity among sulfonucleotide reductases. *ACS Chem. Biol.* **2012**, *7*, 306–315. [[CrossRef](#)]

Disclaimer/Publisher’s Note: The statements, opinions and data contained in all publications are solely those of the individual author(s) and contributor(s) and not of MDPI and/or the editor(s). MDPI and/or the editor(s) disclaim responsibility for any injury to people or property resulting from any ideas, methods, instructions or products referred to in the content.